

This work has been submitted to the IEEE for possible publication. Copyright may be transferred without notice, after which this version may no longer be accessible.

User-Driven Voice Generation and Editing through Latent Space Navigation

Yusheng Tian, *Student Member, IEEE*, Junbin Liu, *Student Member, IEEE*, and Tan Lee, *Member, IEEE*

Abstract—This paper presents a user-driven approach for synthesizing specific target voices based on user feedback rather than reference recordings, which is particularly beneficial for speech-impaired individuals who want to recreate their lost voices but lack prior recordings. Our method leverages the neural analysis and synthesis framework to construct a latent speaker embedding space. Within this latent space, a human-in-the-loop search algorithm guides the voice generation process. Users participate in a series of straightforward listening-and-comparison tasks, providing feedback that iteratively refines the synthesized voice to match their desired target. Both computer simulations and real-world user studies demonstrate that the proposed approach can effectively approximate target voices. Moreover, by analyzing the mel-spectrogram generator’s Jacobians, we identify a set of meaningful voice editing directions within the latent space. These directions enable users to further fine-tune specific attributes of the generated voice, including the pitch level, pitch range, volume, vocal tension, nasality, and tone color. Audio samples are available at <https://myspeechprojects.github.io/voicedesign/>.

Index Terms—Voice generation, voice editing, voice customization, latent space navigation, disentangled edit directions.

I. INTRODUCTION

STATE-OF-THE-ART speech synthesis models show the capability of generating speech in a specific person’s voice using only a few reference recordings [1]–[6]. This technology offers vocally stricken individuals a way to regain their lost voices and speaking ability [7]. By adapting an existing speech synthesis model using the target person’s speech recordings, a synthetic voice that closely resembles the person’s original voice can be created. This personalized voice can be used to generate speech of new content, allowing the person to communicate with others and express his/her thoughts and feelings. However, this approach is clearly not applicable to individuals who do not have prior voice recordings, for example, head and neck cancer survivors.

The present study was initiated with a simple purpose: to help voiceless individuals regain the ability of producing speech in their own voices in the absence of prior recordings. In the case that no physical recording exists, the only trace of a person’s voice lies in the auditory memory of him/herself and probably his/her family members and friends. From a research perspective, this task presents the unique challenge of synthesizing a desired voice that the user can clearly identify and recognize, but for which no reference recording is provided. Apart from replicating a specific target voice, a speech synthesis model with such functionality has other

potential applications, such as customizing voices for virtual characters/avatars.

The task we are considering is in essence a black-box optimization problem: maximizing the perceived similarity between a computer-generated voice and what the user has in mind. The objective function, which involves the user’s perceptual judgement, remains unknown and cannot be directly measured. A parallel can be drawn to sound design [8], [9], where artists use synthesizers to realize specific sounds they envision. Through iterative tweaking and focused listening, sound designers navigate the synthesizer’s parameter space until the output sound matches their desired target. Can we create a parametric voice representation that allows users to search for target voices through iterative refinement of voice-related parameters, mirroring the practices of sound design? To meet this need, the voice representation should be designed with consideration on both efficiency and expressiveness. It should be low-dimensional to facilitate manageable exploration in the parameter space. The representation should also maintain sufficient detail for close approximation of target voices.

Previous studies [10], [11] have explored using human feedback to create voices that match a given face or robot. In these studies, speaker embeddings from pre-trained speaker verification (SV) or text-to-speech (TTS) models are used as parametric representations of voice. These embeddings typically entangle various speaker information—such as timbre, accent and speaking style—in a high-dimensional space. To facilitate user exploration, they are reduced to a few principal components. While this simplified representation is adequate for generating plausible voices for a given face or robot, it may lack the detail needed to recreate a specific voice. In this work, we leverage the neural analysis and synthesis (NANSY) framework [12] to construct a speaker embedding space focused on modelling voice timbre. We will show that this results in a low-dimensional yet sufficiently detailed representation, allowing users to control salient timbre characteristics with a small parameter set. While our focus is on voice timbre, the modular design of NANSY allows for incorporating additional controls over other aspects of speech, such as articulation and speaking style [13].

One way to navigate a parameter space is known as the Gibbs sampling with people [10], [11], [14], where human listeners iteratively manipulate sliding bars, adjusting one parameter dimension at a time to optimize the model output. This trial-and-error process can be tedious and cognitively demanding, especially in our intended application where the evaluation requires listening to audio samples that may sound similar. To reduce the user’s effort, a simple but practical

Yusheng Tian, Junbin Liu and Tan Lee are with the Department of Electronics Engineering, The Chinese University of Hong Kong, Hong Kong SAR of China.

search algorithm is introduced. The search process is broken down into a series of straightforward comparison tasks. Both computer simulations and real-world user studies demonstrate that, with proper initialization, the algorithm can effectively arrive at good approximations of target voices.

After obtaining a target voice, users might want to fine-tune it for various communication needs, e.g., increasing the volume to project confidence or reducing nasal resonance to simulate a stuffy nose. By analyzing the Jacobians of the mel-spectrogram generator, we identify a set of voice editing directions in the latent speaker embedding space. Each direction corresponds to a distinct voice-related attribute: pitch level, pitch range, volume, vocal tension, nasality, and tone color. Users can adjust any of these attributes in the generated voice by perturbing the respective component(s) of the speaker embedding.

The key contributions of this study are summarized as follows:

- A user-driven approach to synthesizing desired voices based on human listeners’ feedback is formulated and investigated thoroughly. Through a sequential process of comparative perceptual evaluation, listeners can iteratively refine a latent voice representation, guiding the synthesis model to generate the desired voices. This approach is particularly valuable to generating speech for vocally stricken individuals who do not have speech recordings for model training.
- Computer simulations and real-world user studies are carried out to demonstrate the effectiveness of the proposed approach in searching and approximating a target voice, starting from a properly initialized voice representation.
- Meaningful voice editing directions in the latent space are identified by analyzing the mel-spectrogram generator’s Jacobians. The editing directions allow users to fine-tune specific attributes of generated voice, enabling flexible control and customization.

II. RELATED WORK

A. Targeted Voice Generation without Reference Recordings

Recent studies on speaker generation [13], [15]–[25] explored methods of generating novel artificial voices without requiring recordings from a new speaker. In these methods, generative models are trained to fit the underlying distribution of voice characteristics and new voices are generated by sampling the learned distribution. While speaker generation models can be conditioned on certain user specifications, e.g., gender, age group [15]–[17], or even detailed textual descriptions like “a low-pitch middle-aged women’s voice with a dark, husky tone” [19]–[21], [23]–[25], they still cannot reliably synthesize highly specific target voices. This limitation might stem from the inherent subjectivity of speech perception and the fact that voice characteristics cannot be adequately described by words. A user’s perception of a “warm” voice, for instance, might not align with the model’s interpretation. A single piece of text description could also potentially be suitable to many different voices.

Another line of research in speaker generation considered the use of human feedback to adjust model parameters to produce a desired voice [10], [11]. These works aimed to create voices perceived as generally plausible for a given face or robot, rather than to match a specific target person’s voice. Thus a less detailed voice representations could be used. Such representation could be obtained by reducing high-dimensional speaker embeddings to a small number of principal components. In our work, the voice representation is desired to be of low-dimension yet sufficiently detailed such that it can capture the nuances of a specific target voice. The approach of Gibbs sampling [14] has been commonly applied to realize human navigation in the voice parameter space. The navigation is done by adjusting parameters on a sliding bar for each dimension. In the present study, a user-friendly navigation process is proposed to implement the search process as a series of straightforward comparison tasks. The comparison-based search process is expected to reduce the user effort as humans are known to excel at comparing options and indicating preferences [26], [27].

B. Attribute Editing within the Latent Space

Attribute editing within latent spaces, particularly those learned by Generative Adversarial Networks (GANs), has been extensively studied in the area of image generation [28]–[40]. It was shown that unsupervised methods could identify meaningful editing directions within the GAN latent space, which correspond to interpretable attribute changes in generated images, such as the gender, makeup, or pose of a generated human face [32]–[40]. A majority of these methods [36]–[40] were grounded on singular value decomposition (SVD) of Jacobian matrices. The underlying hypothesis is that effective editing directions correspond to axes along which changes in the latent code result in the most significant changes in the generator output. In our work, the right singular vectors of the mel-spectrogram generator’s Jacobians are analyzed to discover meaningful voice editing directions within the latent speaker embedding space. We aim to achieve targeted control of voice attributes, analogous to controlling image attributes by manipulating latent representations along specific directions.

III. LATENT SPEAKER EMBEDDING SPACE

In this section, the construction of latent speaker embedding space is described. It is based on the NANSY framework. All subsequent experiments are carried out with this latent space.

A. Framework Overview

NANSY [12] is a framework designed for flexible analysis and (re-)synthesis of speech signals. It decomposes a speech signal into four parts of analysis features, namely pitch, energy, pronunciation and timbre. These features can be independently manipulated and recombined to synthesize a new speech signal which sounds differently from the input signal.

The core analysis-and-synthesis architecture of NANSY as illustrated in Fig.1 is adopted in this study. The input speech waveform is analyzed to extract the four parts of

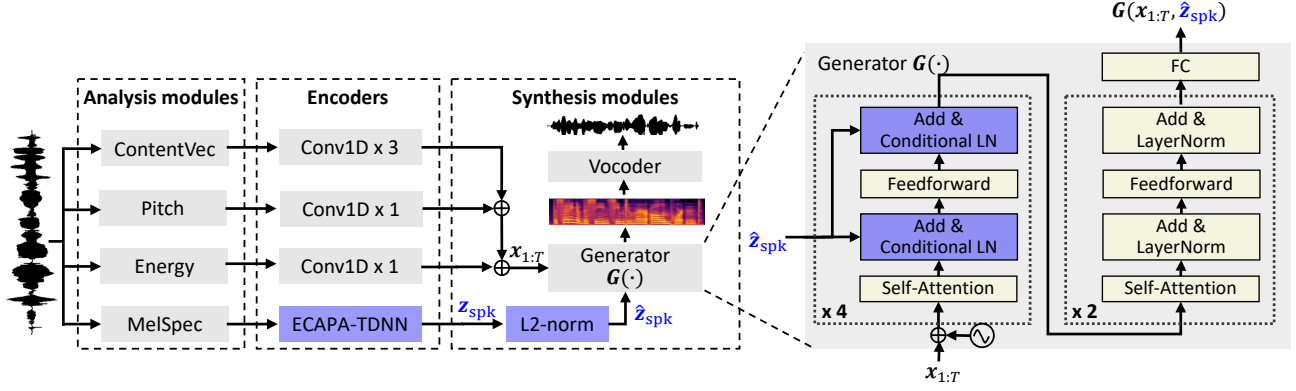


Fig. 1. The modified NANSY framework. The learned speaker embeddings are used to construct the latent space. These embeddings mainly encode pitch, volume and timbre-related information. Pitch and energy features are per-utterance normalized.

speech features, which are subsequently encoded into internal representations. The output speech is synthesized using a HiFi-GAN vocoder [41] from the mel-spectrogram that is reconstructed from the internal representations. The speaker embeddings learned with this framework are used as the parametric voice representation. The original NANSY framework has been modified in a few aspects to suit our needs. First, we use ContentVec [42] instead of wav2vec 2.0 [43] to extract pronunciation-related information. As demonstrated in [42], this model can produce representations that are more closely aligned with phonetic units and less sensitive to speaker variations than the wav2vec, making it particularly suitable to our task. Second, the Yingram is replaced by fundamental frequency values, for explicit pitch control and straightforward extension to text-to-speech applications. Third, in the mel-spectrogram generator, transformer layers are used in place of convolutional layers, because of the superior reconstruction quality demonstrated empirically. Finally, given that the overall pitch and volume are important to characterizing a voice, the pitch features extracted from raw speech waveforms are scaled by the mean value, and the energy features are normalized to have zero mean. In this way the global pitch and volume information are incorporated into the speaker embedding.

B. Implementation Details

1) *Speech feature extraction*: Pitch is measured by the fundamental frequency (F_0) values extracted using the DIO algorithm [44] in the PyWORLD toolkit¹. This F_0 sequence is scaled by its mean value, then encoded into a sequence of 128-dimensional vectors using a 1D convolutional layer. Similarly, energy features, calculated by summing the log mel-spectrogram along the frequency axis, are normalized to have zero-mean and then go through the same encoding process, resulting in another sequence of 128-dimensional vectors. Timbre information is extracted with the ECAPA-TDNN network [45]. It takes 80-dimensional log mel-spectrograms as input and produces 192-dimensional speaker embedding vectors. Following [12], speaker embeddings are normalized to unit

length. Both the mel-spectrogram and F_0 sequence are computed using a window size of 1024 and a hop size of 256 for a 22.05 kHz input speech signal, ensuring compatibility with the HiFi-GAN vocoder. For pronunciation features, we utilize ContentVec with the publicly released pretrained checkpoint. Following [42], the output of the twelfth layer is chosen as the ContentVec feature. ContentVec operates on 16 kHz speech signals, transforming them into sequences of 768-dimensional vector sequences with a 20 ms stride. These features are upsampled to match the length of the F_0 and energy sequences, and then encoded into 128-dimensional vectors with a 3-layer 1D convolutional network.

2) *Speech signal reconstruction*: The encoded pronunciation, pitch and energy features are summed and fed to the mel-spectrogram generator, which consists of six feed-forward transformer blocks, each with a hidden dimension of 128, a feed-forward filter size of 512, a kernel size of 9, and two attention heads. The first four transformer blocks take the L_2 -normalized speaker embedding \hat{z}_{spk} to control the layer normalization in each self-attention and feed-forward network. This conditional layer normalization operation is defined as

$$\text{CondLN}(\mathbf{x}_i, \hat{z}_{\text{spk}}) = \frac{\mathbf{x}_i - \mu(\mathbf{x}_i)}{\sigma(\mathbf{x}_i)} + \mathbf{A}_i \hat{z}_{\text{spk}}, \quad (1)$$

where $\mu(\mathbf{x}_i)$ and $\sigma(\mathbf{x}_i)$ represent the mean and variance of the hidden vector \mathbf{x}_i for the i^{th} layer normalization, and \mathbf{A}_i is a linear layer applied to the length-normalized speaker embedding \hat{z}_{spk} . We find it sufficient to incorporate speaker information through the bias term alone, so that there is no scale vector in (1). The output of the mel-spectrogram generator is then passed to the pretrained Universal HiFi-GAN v1² to synthesize the final speech waveform.

3) *Training*: We train the encoders and mel-spectrogram generator using the LibriTTS-R dataset [46], which is derived by applying speech enhancement to the original multi-speaker speech corpus LibriTTS [47]. To ensure that the speaker encoder can effectively extract speaker information, we select only utterances longer than 2.0 second from the training set (including “train-clean-100”, “train-clean-360”, and “train-other-500”), which correspond to 527 hours of speech data

¹<https://github.com/JeremyCCHsu/Python-Wrapper-for-World-Vocoder>

²<https://github.com/jik876/hifi-gan>

TABLE I
CUMULATIVE EXPLAINED VARIANCE RATIO (%) BY PRINCIPAL COMPONENTS FOR LEARNED SPEAKER EMBEDDINGS

# Principal Components	Female Voices			Male Voices		
	8	16	32	8	16	32
Look-Up Table (VITS)	22.8	34.1	45.2	21.9	32.5	43.4
ECAPA-TDNN (SV)	36.1	54.5	73.0	33.9	51.1	69.3
ECAPA-TDNN (NANSY)	60.5	75.8	89.4	55.5	72.6	87.9

from 2,293 speakers. The model is trained for 200,000 steps on L_1 mel-spectrogram reconstruction loss, using the Adam optimizer with a learning rate of 1e-4 and a batch size of 32. The entire training process takes approximately 42 hours on a single Tesla-V100 GPU.

C. Principal Component Analysis of Speaker Embeddings

To demonstrate the benefits of using NANSY to learn the latent speaker embedding space, we compare speaker embeddings obtained through NANSY to those derived from established TTS and SV models.

For this comparison, we trained a VITS TTS model [48] on LibriTTS-R using the publicly available training script³. We also trained a variant of the NANSY model which employed an ECAPA-TDNN encoder pretrained on speaker verification⁴.

The VITS model represents each of the 2,293 training speakers with a unique 256-dimensional vector stored in a look-up table. In contrast, the two ECAPA-TDNN encoders generate a speaker embedding for each utterance. To facilitate comparison, we averaged the embeddings for each speaker, resulting in 2,293 speaker embeddings from both the pretrained ECAPA-TDNN (SV) and the ECAPA-TDNN (NANSY), all represented as 192-dimensional vectors.

We then performed Principal Component Analysis (PCA) on these speaker embeddings. Female voices and male voices were modelled separately. Table I shows the cumulative explained variance ratio by different numbers of principal components. Notably, ECAPA-TDNN trained jointly with NANSY exhibits a significantly lower-dimensional embedding space than VITS and ECAPA-TDNN (SV). Within this space, the first 32 principal components account for nearly 90% of the total variance. This concise representation is consistent with the model’s primary focus on voice timbre. In contrast, both VITS and ECAPA-TDNN (SV) embeddings encompass a broader range of speaker-specific characteristics such as accents and speaking styles, resulting in higher dimensionality.

How do these principal components relate to voice reconstruction quality? To answer this question, we projected the extracted speaker embeddings onto a reduced set of principal components and evaluated the fidelity of voices reconstructed from these reduced representations. Specifically, for each of the 2,293 speakers, we randomly selected one utterance and generated two reconstructed voices: one using the full-dimensional embedding (z) and another using a reduced-dimensional embedding (\bar{z}). The reduced embedding was

TABLE II
PERCENTAGE OF RECONSTRUCTED VOICES (%) ACHIEVING RESEMBLYZER SIMILARITY SCORE ABOVE THE MEDIAN INTRA-SPEAKER SIMILARITY COMPUTED ACROSS THE DATASET

# Principal Components	Female Voices			Male Voices		
	8	16	32	8	16	32
Look-Up Table (VITS)	72.0	93.7	97.4	69.1	91.3	96.9
ECAPA-TDNN (SV)	92.8	97.0	99.1	90.2	97.3	99.2
ECAPA-TDNN (NANSY)	98.1	99.3	99.8	95.4	99.3	99.9

obtained using the formula: $\bar{z} \leftarrow \mathbf{W}_K \mathbf{W}_K^T (z - \mu) + \mu$, where \mathbf{W}_K represents the matrix containing the first K principal components, and μ is the average speaker embedding. We then measured the similarity between the two reconstructed voices (full-dimension vs. reduced-dimension) using Resemblyzer⁵, a widely adopted open source speaker encoder.

Table II shows the percentage of reconstructed voices that, when compared to their full-dimensional versions, achieve a similarity score above 0.85. This threshold corresponds to the median intra-speaker similarity across the dataset, representing a high degree of similarity according to Resemblyzer. Notably, speaker embeddings from the two ECAPA-TDNN encoders, with only the first eight principal components, can reconstruct voices exceeding this similarity threshold for over 90% of the speakers, significantly outperforming VITS embeddings. This difference in reconstruction efficiency could be due to their distinct speaker encoding mechanisms. Unlike VITS, which represents speakers in isolation, ECAPA-TDNN directly extracts speaker information from speech utterances, resulting in speaker embeddings that effectively capture acoustic similarities and variations between different voices.

While the pretrained ECAPA-TDNN (SV) shows similar efficiency to the jointly trained ECAPA-TDNN (NANSY) in modelling voice characteristics, its embedding space lacks the same level of organization. Specifically, in the NANSY-derived embedding space, only the first three principal components exhibit a strong correlation with pitch variations. In contrast, in the SV-derived embedding space, shifting the speaker embedding along a majority of nonconsecutive principal directions leads to noticeable pitch changes. This more organized structure within the NANSY-derived embedding space could potentially simplify user exploration. Readers are encouraged to visit the demo page to hear these differences.

IV. SEARCHING FOR THE TARGET VOICE

A. Problem Formulation

Applying PCA to the learned speaker embeddings yields a set of principal directions. We select the first N of these directions and denote them as $\mathbf{w}_1, \mathbf{w}_2, \dots, \mathbf{w}_N$. Any speaker embedding z can be approximated by projecting it onto the subspace spanned by these selected principal directions:

$$z \approx \mathbf{W}\alpha + \mathbf{b}, \quad (2)$$

³<https://github.com/jaywalnut310/vits>

⁴<https://huggingface.co/speechbrain/spkrec-ecapa-voxceleb>

⁵<https://github.com/resemble-ai/Resemblyzer>

where $\alpha = [\alpha_1, \alpha_2, \dots, \alpha_N]^T$ represents the linear combination coefficients, and $\mathbf{W} = [\mathbf{w}_1, \mathbf{w}_2, \dots, \mathbf{w}_N]$ represents the basis matrix of the subspace, and \mathbf{b} is an offset vector. By fixing \mathbf{b} to a predefined value (e.g. the average speaker embedding), our goal becomes optimizing the N coefficients α to maximize the user’s perceptual preference for the generated voice. This leads to the following optimization problem:

$$\max_{\alpha \in \mathbb{R}^N} f \circ V \circ G \left(\frac{\mathbf{W}\alpha + \mathbf{b}}{\|\mathbf{W}\alpha + \mathbf{b}\|} \right), \quad (3)$$

where functions $G(\cdot)$, $V(\cdot)$, and $f(\cdot)$ represent the mel-spectrogram generator, the vocoder, and the user’s perceptual preference function (which is unknown), respectively. The normalization step within the equation reflects the process of normalizing the speaker embedding to unit length before feeding it to the generator for speech generation.

B. Search Algorithm

The objective function in (3) includes a perceptual judgement that cannot be directly modelled. We therefore employ a human-in-the-loop approach. Our search algorithm draws inspiration from coordinate descent [49], an iterative method for optimizing multivariate functions. Coordinate descent operates by sequentially optimizing one variable at a time while holding the others fixed, and cycling through all variables repeatedly until convergence. Similarly, the proposed approach decomposes the optimization process into a series of one-dimensional optimizations along each principal direction. Each of these one-dimensional optimizations is guided by user feedback, incorporating human perception into the search process.

The search process begins with an initial estimate of the target voice, e.g., the average female or male speaker embedding calculated from the training dataset. To explore potential variations, this initial estimate is systematically perturbed along one principal direction, generating a set of candidate speaker embeddings. Each candidate embedding is then normalized to unit length and passed to the mel-spectrogram generator to synthesize a corresponding audio sample. The user listens to these audio samples and selects the most preferable one. The chosen candidate then becomes the starting point for the next iteration, which explores variations along a different principal direction. This process continues, traversing all principal directions repeatedly until the user identifies a satisfactory voice or a predefined maximum number of iteration is reached.

Algorithm 1 summarizes the proposed search algorithm. Line 5 and 6 describe the generation of candidate voices using a progressively refined search strategy: the distance between candidates is decreased by half after each cycle. Line 7 outlines the user interaction for candidate selection.

Fig. 2 illustrates how user responses guide the search process. For evaluation purposes, the user interface shown in Fig. 2 includes a reference voice, and participants are asked to select a candidate voice most similar to it. This setup allows us to assess how closely the search result matches the target voice. In real-world use, however, the interface should not include the reference. Users are expected to rely entirely on

Algorithm 1 User-driven search for the target voice

Require: N principal directions $\mathbf{w}_1, \mathbf{w}_2, \dots, \mathbf{w}_N$

Require: N step sizes d_1, d_2, \dots, d_N

Require: Initialization voice $\mathbf{z}^{(0)} = \mathbf{W} \cdot \mathbf{0} + \mathbf{b}$

```

1:  $i \leftarrow 0$ 
2: while stopping criteria is not met do
3:    $n \leftarrow i \bmod N + 1$   $\triangleright$  principal direction index
4:   for  $k = \pm 1, \pm 2, 0$  do
5:      $\mathbf{z}_k^{(i)} \leftarrow \mathbf{z}^{(i)} + k \cdot 2^{-\lfloor \frac{i}{N} \rfloor} d_n \mathbf{w}_n$   $\triangleright$  candidate voices
6:   end for
7:    $\mathbf{z}_{\text{sel}}^{(i)} \leftarrow \arg \max f \circ V \circ G \left( \frac{\mathbf{z}_k^{(i)}}{\|\mathbf{z}_k^{(i)}\|} \right)$   $\triangleright$  user response
8:    $\mathbf{z}^{(i+1)} \leftarrow \mathbf{z}_{\text{sel}}^{(i)}$ 
9:    $i \leftarrow i + 1$ 
10: end while

```

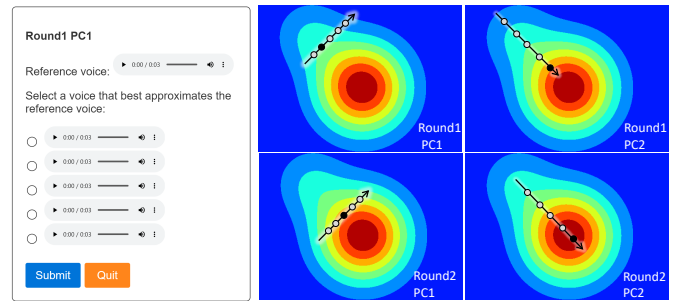


Fig. 2. Illustration of the search process. Left: the user interface for a single query. Users are presented with a set of voices and asked to select the one most similar to their target. Right: an example optimization sequence within a 2-dimensional search space. Each iteration involves generating candidate voices by systematically varying the parameter along one principal direction. The user’s selection then defines the starting point for generating candidates along the next principal direction. This iterative process of comparison progressively guides the search towards the target.

their mental representation of the desired voice to make their choices.

C. Synthetic Simulation for Hyperparameter Tuning

The proposed search algorithm is configured with two sets of hyperparameters: 1) the number of selected principal directions (N), which defines the dimensionality of the search space; and 2) the step size along each principal direction (d_1, d_2, \dots, d_N), which controls the generation of candidate voices. Determining optimal values of these hyperparameters in the human-in-the-loop setting would be prohibitively time-consuming and labor-intensive. To address this issue, we propose a simulation approach which incorporates a surrogate objective function to guide an automatic process of hyperparameter tuning.

Desirably the surrogate function should effectively reflect human perceptual judgments of voice similarity. To achieve this, a heuristic approach is proposed by combining multiple loss functions to approximate human perception. The rationale is that a combination of diverse losses can mitigate individual biases and provide a more comprehensive representation of human perception. The proposed objective function incorporates the standard mean squared error (MSE) loss on the

log mel-spectrogram, and voice similarity scores measured by two pretrained speaker verification models (Resemblyzer and ECAPA-TDNN). Given a reference speech signal \mathbf{y}^{ref} , and a speaker embedding \mathbf{z} to be evaluated, the surrogate objective function is defined as:

$$\begin{aligned} S(\mathbf{z}) = & -\text{MSELoss}(\mathbf{y}_{\text{mel}}(\mathbf{z}), \mathbf{y}_{\text{mel}}^{\text{ref}}) \\ & + \text{Resemblyzer_Score}(\mathbf{y}_{\text{wav}}(\mathbf{z}), \mathbf{y}_{\text{wav}}^{\text{ref}}) \\ & + \text{ECAPA-TDNN_Score}(\mathbf{y}_{\text{wav}}(\mathbf{z}), \mathbf{y}_{\text{wav}}^{\text{ref}}), \end{aligned} \quad (4)$$

where $\mathbf{y}_{\text{mel}}(\mathbf{z})$ is the reconstructed mel-spectrogram, obtained by replacing the original speaker embedding with \mathbf{z} while keeping other speech features unchanged. $\mathbf{y}_{\text{wav}}(\mathbf{z})$ is the corresponding speech waveform generated using the HiFi-GAN vocoder.

The simulation pipeline proceeds as follows. For each speech sample of a target voice, an average speaker embedding (calculated separately for male and female voices from the entire LibriTTS-R training dataset) is applied to provide an initial estimate of the target voice. The simulation then executes the search process detailed in Algorithm 1, with the surrogate objective function imitating human decision-making in line 8. The search process is designed to terminate after 32 queries, which reflects the limitation of real user evaluation.

To evaluate the performance of our search algorithm under various hyperparameter settings, we conducted simulations using diverse target voices and measured the resulting voice similarity with Resemblyzer. Specifically, we randomly sampled one utterance from each speaker in the LibriTTS-R test sets (“test-clean” and “test-other”) and the VCTK [50] dataset (for out-of-domain evaluation). This yielded 72 unique target voices from LibriTTS-R and 110 from VCTK. For each target voice, we carried out simulations with varying numbers of principal directions ($N = 8, 16, 32$) and step sizes ($d_i = 0.5\sigma_i, \sigma_i, 2\sigma_i$), where σ_i denotes the standard deviation of speaker embeddings projected onto the i^{th} principal direction.

The extensive simulations revealed that the search algorithm is quite robust to changes in step size, as voice similarity scores remained relatively consistent across the tested values. However, the number of principal components significantly impacted the achieved similarity. Increasing the number of principal components consistently led to more substantial improvements in similarity compared to performing additional search iterations with fewer components, as illustrated in Fig.3. Note that cycling through 8 principal directions 4 times proved less effective than a single cycle through 32 principal directions. By examining audio samples selected by the surrogate objective function, it is found that the differences between candidate voices became imperceptible to human listeners beyond 16 principal directions. Based on these findings, we set $N = 16$, $d_i = \sigma_i$ for $i = 1, \dots, N$ for all subsequent experiments.

D. Human Evaluation of Simulation Results

While Resemblyzer scores provide guidance for hyperparameter tuning, their numerical scale does not directly translate to human perception of voice similarity. We therefore carried out subjective listening tests to evaluate the simulated

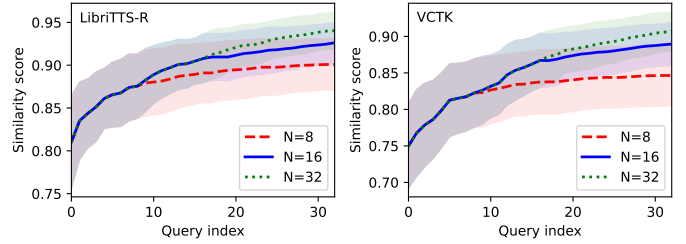


Fig. 3. Voice similarity scores, as measured by Resemblyzer, across consecutive queries of simulated search processes. The simulations investigate the impact of varying the number of principal components on the achieved voice similarity, with the step size fixed at $d_i = \sigma_i$. Solid lines represent the mean scores over all target voices for each query, and the shaded regions depict the standard deviation.

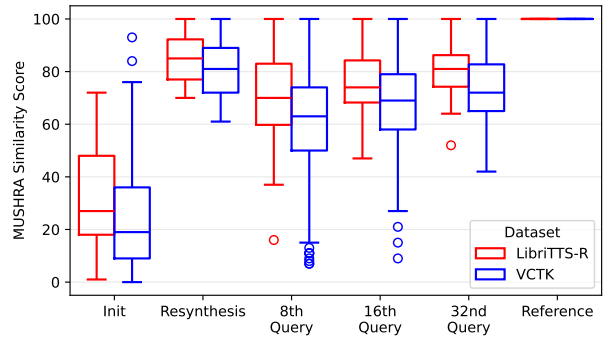


Fig. 4. Results of MUSHRA-style listening tests evaluating the perceived similarity of simulated search results to target voices. The box plot displays the distribution of similarity scores for: the initialization voice; the NANSY-resynthesized voice; candidate voices selected at different stages of the simulated search process; and the original target voice (reference). The box represents the interquartile range (IQR), with the embedded line indicating the median. Whiskers extend to the furthest data points within 1.5 times the IQR, and outliers beyond this range are plotted as individual circles.

search results. These tests focused on a subset of 67 target voices (17 from LibriTTS-R and 50 from VCTK) with initial Resemblyzer similarity scores below 0.75. We hypothesized that voices with lower initial similarity would prove more challenging for the algorithm and thus more informative for evaluating its effectiveness.

The listening test was in MUSHRA-style format. For each target voice, listeners were presented with six stimuli: the candidate voices selected at the 8th, 16th, and 32nd queries of the simulated search process; the initialization voice; the NANSY-resynthesized voice; and the original target voice recording (also served as the reference). Listeners rated the similarity of each stimulus to the reference on a scale of 0 to 100, with scores above 60 and 80 considered “good” and “excellent” similarity, respectively. Listeners were instructed to assign a score of 100 to at least one stimulus. To maintain a manageable test duration (around 15 minutes), each listener was randomly presented with 10 out of the 67 test cases. We recruited participants from the university and received 24 valid responses, defined as those successfully identified the original recording and rated it as 100.

Fig. 4 shows the results. While a performance drop is evident when synthesizing out-of-domain voices from VCTK, all NANSY-resynthesized voices achieved at least “good” sim-

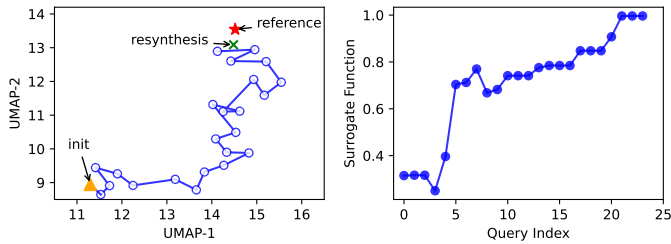


Fig. 5. A typical user session. Left: UMAP-projected speaker embeddings, extracted using Resemblyzer, show how the user’s selected voice progressively approaches the reference voice after each query. Right: Similarity scores calculated using the surrogate objective function indicate a general agreement between the surrogate function and human preferences.

ilarity to their targets. This suggests that the constructed latent speaker embedding space consistently provides a reasonable approximation of unseen voices. Notably, for over half of the target voices, the simulated search process converged to a good approximation within the first cycle (by 16th query), and over 75% reached a good match by the final query (32nd). The next subsection details our investigation into cases where the search process did not yield a good match, drawing on insights from in-depth user studies.

E. User Study

To evaluate the real-world performance of our search algorithm, we conducted a user study guided by two key questions. First, we wanted to determine whether human preferences align with the results produced by the simulated search, particularly in cases where the simulation achieved high similarity scores. Second, we aimed to understand why the simulated search struggled in certain scenarios, and investigate whether human users would encounter similar difficulties.

For this study, we carefully selected two sets of target voices. The first set, representing “easy” scenarios, consisted of one female and one male voice where the simulated search achieved the highest listening test scores. The second set, representing “hard” scenarios, comprised the five target voices for which the simulated search failed to produce a good approximation (i.e., achieved listening test scores below 60).

Our preliminary experiments revealed that initializing the search with the most similar voice from the training data, rather than the average voice, often led to improved voice similarity, particularly in “hard” scenarios. Building on this finding, we designed the user study to include two initialization settings: “average initialization” (starting with the average voice) and “optimal initialization” (starting with the most similar voice from the training data).

Twenty-one participants from the university community completed the user study, which was conducted through a web interface. Each participant was randomly assigned one of the seven target voices, with three participants assigned to each voice. Before the formal test trials, participants completed a training trial to familiarize themselves with the procedure and user interface. During the formal trials, participants were allowed to have three attempts to reach their assigned target voice using each initialization setting (“average initialization”

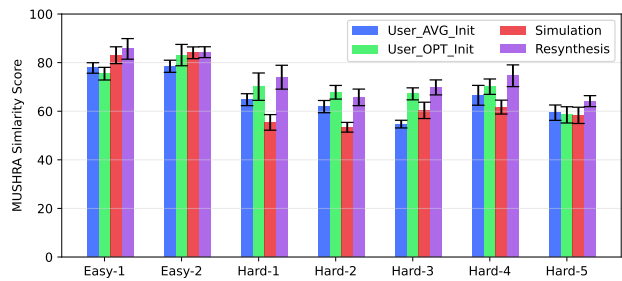


Fig. 6. Results of the MUSHRA-style listening test for the user study, grouped by target voices. The bar graph displays the average score, with error bars indicating the 95% confidence interval.

and “optimal initialization”), resulting in a total of six attempts per target voice. For each initialization setting, only the attempt that the participant subjectively rated as the closest match to the target voice was kept for analysis.

Fig. 5 illustrates a typical user session for an “easy” target voice. While the UMAP-projected search trajectory and the similarity scores measured by the surrogate objective function exhibit some fluctuation, the overall trend demonstrates increasing similarity as the search progresses, indicating a general agreement between the surrogate objective function and human preferences.

We then conducted a MUSHRA-style listening test, similar to the previous evaluation, to assess the perceived similarity of the voices produced in the user study. For each target voice, listeners evaluated five stimuli: the user-searched results obtained with both average and optimal initialization; the simulated search result; the directly resynthesized voice; and the original target voice recording (also serving as the reference). Each listener completed seven questions, one for each target voice. The user-searched results for each question were randomly selected from the three corresponding user study trials. We collected 20 valid responses after excluding those who failed to identify the hidden reference.

Fig. 6 presents the listening test results. In the two “easy” cases, user-searched voices achieved near-excellent similarity to the target, regardless of the initialization method. This contrasts with the five “hard” cases, where achieving high similarity proved more challenging. The performance gap between “easy” and “hard” cases is consistent with our earlier simulated search results.

Interestingly, in “Hard-1” and “Hard-2”, user-searched results using simple average initialization significantly outperformed the results generated by the simulated search. We speculate this to stem from a mismatch between the surrogate objective function and human perception of similarity.

A closer look at the five “hard” scenarios, which proved challenging for both the simulated search and users, revealed two key factors that led to inferior performance.

1) *Sub-optimal initialization*: This factor is evident in most “hard” scenarios (from “Hard 1” to “Hard 4”), where user searches consistently achieved better similarity when initialized with the most similar voice from the training data (optimal initialization). To quantify the benefit of optimal initialization, we analyzed listener preferences. For each simulation setting,

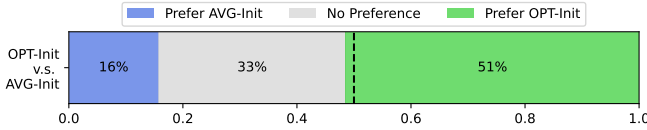


Fig. 7. Listener preferences for initialization methods in the MUSHRA-style listening test for user-searched results.

a preference was recorded if a listener rated the result from one initialization method at least 5 points higher than the other. Fig.7 aggregates these preferences across all listening test responses, clearly demonstrating that optimal initialization leads to higher listener satisfaction compared to average initialization.

2) *Out-of-domain targets*: “Hard 5” highlights the challenge posed by out-of-domain target voices. In this scenario, both simulated and user-driven searches exhibited a noticeable performance drop, regardless of the initialization method used. Even the best user-searched result barely surpassed the threshold for “good” similarity. This limitation appears to arise from the resynthesized voice itself, which achieved a similarity score just above 60. This suggests that the primary obstacle lies not in the search algorithm’s ability to find a good match, but rather in the limited representation of such out-of-domain voices within the latent space. We anticipate that incorporating a larger, more diverse dataset during the construction of the speaker embedding space would lead to improved performance for both simulated and user-driven searches when targeting these challenging voices.

V. VOICE EDITING DIRECTIONS

While our initial analysis of the speaker embedding space did not reveal clearly interpretable directions for voice editing, we observed that the first three principal components corresponded to pitch manipulation. This suggests that directions capable of controlling specific voice attributes might exist within the latent space. To explore this possibility, we adapt techniques from the image domain to uncover voice editing directions within the latent speaker embedding space.

A. Unsupervised Discovery of Voice Editing Directions

Given a speech sample, let \mathbf{z} be its speaker embedding and $\mathbf{x}_{1:T}$ be the other speech features extracted within the NANSY framework. Using the mel-spectrogram generator $G(\cdot)$, we can reconstruct the speech signal from these inputs.

To investigate how the speaker embedding influences the generated voice, perturbations are applied to \mathbf{z} along specific directions. The instantaneous change in the generated mel-spectrogram resulting from a change in the speaker embedding \mathbf{z} along a direction \mathbf{v} is given by

$$\lim_{\epsilon \rightarrow 0} \frac{\tilde{G}_{\mathbf{x}}(\mathbf{z} + \epsilon \cdot \mathbf{v}) - \tilde{G}_{\mathbf{x}}(\mathbf{z})}{\epsilon} = J_{\tilde{G}_{\mathbf{x}}}(\mathbf{z}) \cdot \mathbf{v}, \quad (5)$$

where $\tilde{G}_{\mathbf{x}}(\mathbf{z}) = G\left(\frac{\mathbf{z}}{\|\mathbf{z}\|}, \mathbf{x}_{1:T}\right)$, and $J_{\tilde{G}_{\mathbf{x}}}(\mathbf{z})$ is the Jacobian of $\tilde{G}_{\mathbf{x}}$ evaluated at \mathbf{z} .

A common assumption in GAN latent space analysis, supported by several previous studies [36], [38]–[40], is that

effective editing directions should cause the most significant changes in the generated output. Guided by this principle, we search for voice editing directions that maximize the magnitude of change in the generated output, as quantified by Equation (5). Knowledge in matrix analysis [51] tells us that these directions correspond precisely to the leading right singular vectors of the Jacobian matrix $J_{\tilde{G}_{\mathbf{x}}}(\mathbf{z})$.

We explicitly choose to compute the Jacobian from the generated mel-spectrogram, rather than from the raw speech waveform or internal hidden layer outputs. This choice is motivated by the fact that the mel-spectrogram, designed to approximate human auditory perception, provides a more perceptually relevant representation for identifying voice editing directions.

Our initial experiments confirm that this method yields directions that produce distinct and interpretable changes in voice attributes (e.g., pitch, volume, vocal tension) for individual speech samples. Importantly, while these directions are specific to individual utterances, we observe that *certain directions generalize across utterances, even for different speakers or content*. This suggests the potential existence of a common set of voice editing directions applicable to any speaker embedding within the latent space, regardless of the speaker or speech content.

To test this hypothesis, we designed an experiment using the LibriTTS-R dataset. We selected one utterance from each speaker in both the training and development sets. For each utterance, we computed the Jacobian matrix of the reconstructed mel-spectrogram with respect to the speaker embedding. We then extracted the top 32 right singular vectors from each Jacobian matrix, yielding a set of candidate editing directions for each utterance.

Next, to determine if any of these candidate directions generalize across utterances, we applied DBSCAN clustering [52] to the extracted vectors, using cosine similarity as the distance metric with a threshold of 0.1. We chose DBSCAN for its ability to filter out noise vectors that do not belong to any cluster. The geometric center of each resulting cluster was then selected as a shared voice editing direction.

We empirically found that using normalized speaker embeddings to compute the Jacobian matrices resulted in more clusters, and thus more of these shared voice editing directions. This clustering process was performed separately for directions extracted from female and male voices. Interestingly, this yielded six distinct editing directions for each gender, with one direction shared between genders.

B. Interpreting Discovered Voice Editing Directions

To determine the voice attributes associated with these editing directions, we manually examined several utterances, varying their speaker embeddings along each direction and listening for changes in the synthesized voice. Our examination suggests that the single direction shared between genders controls volume, while the other five influence the distribution of energy across different frequencies, affecting attributes like pitch and nasalization. This finding could explain why the remaining five directions are gender-specific, as male and female voices naturally possess distinct frequency characteristics.

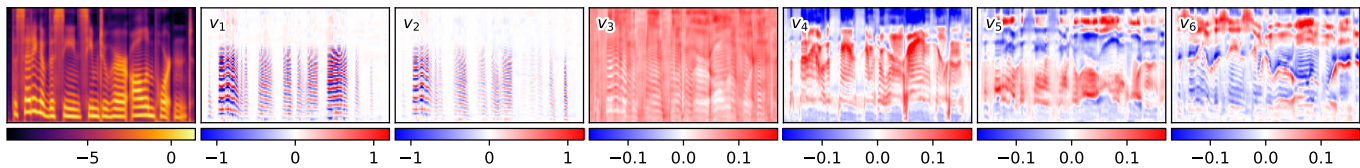


Fig. 8. Visualization of how the generated mel-spectrogram changes when the speaker embedding is shifted along the six principal voice editing directions. The selected speech sample is 6345_93302_000037_000003.wav from the LibriTTS-R dev-clean set, a female voice speaking “The setting of the scene seemed to her all important”. The leftmost plot displays the original mel-spectrogram for reference. The remaining plots show gradient maps, i.e., representations of the directional gradient along each voice editing direction, as calculated using Equation (5).

Figure 8 provides a concrete example, illustrating how the generated mel-spectrogram of a sample utterance changes when the speaker embedding is shifted along each of the six voice editing directions. As the figure demonstrates, each direction induces distinct modifications to the mel-spectrogram.

For example, moving the speaker embedding along the first direction appears to erase the original horizontal stripes in the mel-spectrogram and redraw them at a slightly higher frequency. This suggests that this direction primarily controls the pitch level of the generated voice. The second direction also induces an upward shift in frequency bands but does so selectively, primarily affecting time windows where the fundamental frequency is already high. This targeted manipulation results in increased pitch variation rather than a uniform pitch shift. These two directions are also highly correlated with the top three principal directions discovered by PCA.

Perturbing the speaker embedding along the third direction increases energy across the entire mel-spectrogram, indicating that this direction controls the overall volume. The fourth direction, on the other hand, concentrates added energy within the main body of the frequency bands, a change that corresponds to increased vocal tension or strain.

The effects of the last two directions are less apparent from visual inspection of the gradient maps alone. However, upon listening to the manipulated utterances, we observe that the fifth direction controls the level of nasality in the voice, while the sixth direction affects the overall timbre, shifting a bright voice towards a more muffled quality.

C. Voice Editing Quality

While our initial manual examination of several utterances provides insights into the potential voice editing effects of each identified direction, we need to determine if these effects generalize across a wider range of utterances. To evaluate this, we conducted a formal listening test.

We began by randomly selecting one utterance from each speaker in both the “test-clean” and “test-other” subsets of LibriTTS-R, resulting in a total of 72 utterances (37 female voices and 35 male voices). For each utterance, we used Equation (6) to create two manipulated versions: one where the speaker embedding was shifted toward the editing direction (z_i^+) and one where it was shifted against the direction (z_i^-). The vector v_i in Equation (6) represents the i^{th} editing direction, and parameter σ_i represents the standard deviation of speaker embeddings projected onto that direction.

$$z_i^+ = z + 4\sigma_i v_i, \quad z_i^- = z - 4\sigma_i v_i, \quad i \in \{1 \dots 6\}. \quad (6)$$

	v_1	v_2	v_3	v_4	v_5	v_6
low pitch high pitch	0.95	0.84	0.07	0.05	0.05	0.04
flat expressive	0.06	0.56	0.05	0.01	0.02	0.02
low vol high vol	0.01	0.01	0.88	0.32	0.05	0.02
relaxed strained	0.09	0.06	0.05	0.89	0.06	0.04
less nasal more nasal	0.06	0.02	0.06	0.09	0.59	0.16
bright muffled	0.08	0.04	0.10	0.10	0.46	0.82
no difference	0.00	0.06	0.03	0.01	0.06	0.02

Fig. 9. Listener responses of their perceived changes in voice attributes when the speaker embedding was manipulated along a specific editing direction. Each column represents one of the six editing directions, and the number in each block indicates the percentage of utterances where listeners perceived a noticeable change in the corresponding voice attribute.

We then developed a web-based listening test where each question presented listeners with a pair of these manipulated utterances. This yielded a total of 432 unique questions (6 editing directions \times 72 utterances). Each listening test survey included a random subset of seven questions. Given that nasality is a more subtle and challenging attribute to perceive, two questions focused on this attribute, while the remaining five questions each targeted one of the other voice editing directions.

For each question, listeners were asked to identify any noticeable changes in voice attributes between the two audio samples. The answer choices included descriptions of the six identified effects (volume, pitch level, pitch variation, vocal tension, nasality, and tone color), a “no difference” option, and a free-response option for listeners to describe any perceived changes not captured by the provided choices.

Since the listening test emphasized on identifying subtle differences between voices, we recruited participants via social media, targeting individuals with backgrounds in phonetics or speech and audio processing. Our final participant pool comprised 42 individuals: 11 postgraduate students specializing in speech and audio processing and 31 postgraduate students or graduates with backgrounds in phonetics and phonology. Each participant was allowed to take the listening test a maximum of three times. We ultimately received 116 responses, ensuring each question was evaluated by at least one or two listeners.

TABLE III

TOP-3 MOST FREQUENT LISTENER COMMENTS FOR EACH OF THE SIX EDITING DIRECTIONS. THE TOTAL FREQUENCY OF COMMENTED UTTERANCES ARE INDICATED ON THE LEFT.

Top-3 Most Frequent Listener Comments	
v_1 (3.4%)	deep(25%), resonant(25%), smooth-raspy(25%)
v_2 (5.1%)	monotone(66.7%), smooth-raspy(16.7%), young-old(16.7%)
v_3 (0.0%)	N/A
v_4 (10.3%)	hard glottal attack(50.0%), breathy(16.7%), soft(8.3%)
v_5 (12.9%)	front-back(33.3%), stuffy nose(20.0%), muddy(13.3%)
v_6 (18.9%)	thin-solid(45.4%), slim-fat(13.6%), female-male(9.1%)

Figure 9 summarizes the listener responses with a heatmap, where each column corresponds to one editing direction and each row represents a distinct voice attribute. The prominent diagonal highlights confirm that each editing direction consistently induces the intended voice attribute change, supporting our initial observations from manually examining a smaller set of utterances. However, we also observe some overlap between the perceived effects of v_5 and v_6 , indicating some potential listener confusion between the two dimensions. This overlap could arise because nasality also influences the perceived tone color, and that subtle changes in nasality are more challenging for listeners to identify, compared to other more salient voice attributes.

While listeners were generally able to identify the intended voice attribute changes using the provided multiple-choice options, a subset of utterances prompted additional comments, as summarized in Table III. This table lists the top three most frequent listener comments for each voice editing direction. We manually merged comments that share similar meanings before counting their frequency.

Most comments directly reflect the intended editing effect. For instance, listeners often described low-pitched voices as “deep”, and strained voices as exhibiting “hard glottal attacks”. Some comments point to broader perceptual associations. Nasal voices, for example, gave the impression of producing sounds further back in the vocal tract, while muffled voices, characterized by decreased high-frequency components, were often associated with male voices. A few comments, such as those describing voices as “raspy”, are not directly related to the targeted voice attribute. This suggests the disentanglement between editing effects might be imperfect, leading to unintended secondary effects. Nonetheless, the generally close alignment between the intended voice attributes and listener perceptions suggests that these editing vectors can effectively manipulate a range of salient voice features.

VI. CONCLUSION AND DISCUSSION

We have presented a user-driven approach for generating specific target voices without relying on reference recordings. The proposed approach leverages the user’s familiarity with their desired target voice, guiding them through a series of straightforward comparison tasks to navigate a latent speaker embedding space. The latent speaker representation is designed to be both low-dimensional and sufficiently detailed,

ensuring that users can effectively locate their target voices within a manageable number of attempts. Moreover, we have identified a set of distinct voice editing directions within the latent space. These directions enable users to fine-tune specific voice attributes of the generated voice by simply shifting their searched embeddings along the corresponding editing direction. Extensive user studies and subjective listening tests have demonstrated the effectiveness of the proposed approach for both targeted voice generation and voice attribute editing.

The quality of the search results in the proposed approach depends on the initialization of the search starting point. Our experiments have shown that initializing the search with a voice similar to the target voice often leads to higher similarity between the final search result and the intended target. However, we have not yet explored methods for obtaining such optimal initialization. In future work, we plan to investigate two potential methods: (1) leveraging the recent prompt-based voice generation models to generate an initial voice from user’s textual description of their target, and (2) developing human-in-the-loop algorithms for users to efficiently identify the closet matching voice within a database of voices.

This work focuses on English, leveraging the availability of a large, multi-speaker speech dataset to construct a latent speaker embedding space that represents diverse voices. However, such extensive datasets are often lacking for lower-resource languages. In the future, we aim to extend our approach to multilingual settings, enabling similar voice generation and editing capabilities for languages with limited data resources.

ACKNOWLEDGMENT

The authors would like to thank all the participants in the listening tests and user studies. Their patience, efforts and valuable contributions are essential to this work.

REFERENCES

- [1] S. Ö. Arik, J. Chen, K. Peng, W. Ping, and Y. Zhou, “Neural voice cloning with a few samples,” in *Annu. Conf. Neural Inf. Process. Syst.*, 2018, pp. 10040–10050.
- [2] Y. Jia, Y. Zhang, R. J. Weiss, Q. Wang, J. Shen, F. Ren, Z. Chen, P. Nguyen, R. Pang, I. López-Moreno, and Y. Wu, “Transfer learning from speaker verification to multispeaker text-to-speech synthesis,” in *Annu. Conf. Neural Inf. Process. Syst.*, 2018, pp. 4485–4495.
- [3] Y. Taigman, L. Wolf, A. Polyak, and E. Nachmani, “Voiceloop: Voice fitting and synthesis via a phonological loop,” in *Proc. Int. Conf. Learn. Represent.*, 2018.
- [4] M. Chen, X. Tan, B. Li, Y. Liu, T. Qin, S. Zhao, and T. Liu, “Adaspeech: Adaptive text to speech for custom voice,” in *Proc. Int. Conf. Learn. Represent.*, 2021.
- [5] Y. Wu, X. Tan, B. Li, L. He, S. Zhao, R. Song, T. Qin, and T. Liu, “Adaspeech 4: Adaptive text to speech in zero-shot scenarios,” in *Proc. Interspeech*, 2022, pp. 2568–2572.
- [6] Z. Ju, Y. Wang, K. Shen, X. Tan, D. Xin, D. Yang, Y. Liu, Y. Leng, K. Song, S. Tang, Z. Wu, T. Qin, X. Li, W. Ye, S. Zhang, J. Bian, L. He, J. Li, and S. Zhao, “Naturalspeech 3: Zero-shot speech synthesis with factorized codec and diffusion models,” *CoRR*, vol. abs/2403.03100, 2024.
- [7] J. Mertl, E. Žáčková, and B. Řepová, “Quality of life of patients after total laryngectomy: the struggle against stigmatization and social exclusion using speech synthesis,” *Disabil. Rehabil.: Assist. Technol.*, vol. 13, no. 4, pp. 342–352, 2018.
- [8] M. Russ, *Sound synthesis and sampling*. United States: Taylor & Francis Group, 2012.

- [9] E. R. Miranda and E. R. Miranda, *Computer sound design : synthesis techniques and programming*, 2nd ed., ser. Music technology series. Oxford: Focal Press, 2002.
- [10] P. van Rijn, S. Mertens, D. Schiller, P. Dura, H. Siuzdak, P. M. C. Harrison, E. André, and N. Jacoby, “Voiceme: Personalized voice generation in TTS,” in *Proc. Interspeech*, 2022, pp. 2588–2592.
- [11] P. van Rijn, S. Mertens, K. Janowski, K. Weitz, N. Jacoby, and E. André, “Giving robots a voice: Human-in-the-loop voice creation and open-ended labeling,” in *Proc. CHI Conf. Human Factors Comput. Syst.*, 2024, pp. 584:1–584:34.
- [12] H. Choi, J. Lee, W. Kim, J. Lee, H. Heo, and K. Lee, “Neural analysis and synthesis: Reconstructing speech from self-supervised representations,” in *Annu. Conf. Neural Inf. Process. Syst.*, 2021, pp. 16251–16265.
- [13] H. Choi, J. Yang, J. Lee, and H. Kim, “NANSY++: unified voice synthesis with neural analysis and synthesis,” in *Proc. Int. Conf. Learn. Represent.*, 2023.
- [14] P. M. C. Harrison, R. Marjich, F. Adolphi, P. van Rijn, M. Anglada-Tort, O. Tchernichovski, P. Larrouy-Maestri, and N. Jacoby, “Gibbs sampling with people,” in *Annu. Conf. Neural Inf. Process. Syst.*, 2020.
- [15] D. Stanton, M. Shannon, S. Mariooryad, R. J. Skerry-Ryan, E. Battenberg, T. Bagby, and D. Kao, “Speaker generation,” in *Proc. IEEE Int. Conf. Acoust., Speech Signal Process.*, 2022, pp. 7897–7901.
- [16] P. Bilinski, T. Merritt, A. Ezzerg, K. Pokora, S. Cygert, K. Yanagisawa, R. Barra-Chicote, and D. Korzekwa, “Creating new voices using normalizing flows,” in *Proc. Interspeech*, 2022, pp. 2958–2962.
- [17] Y. Shi and M. Li, “Voicelens: Controllable speaker generation and editing with flow,” *arXiv preprint arXiv:2309.14094*, 2023.
- [18] F. Lux, P. Tilli, S. Meyer, and N. T. Vu, “Controllable generation of artificial speaker embeddings through discovery of principal directions,” in *Proc. Interspeech*, 2023, pp. 4788–4792.
- [19] Z. Guo, Y. Leng, Y. Wu, S. Zhao, and X. Tan, “Prompttts: Controllable text-to-speech with text descriptions,” in *Proc. IEEE Int. Conf. Acoust., Speech Signal Process.*, 2023, pp. 1–5.
- [20] Y. Leng, Z. Guo, K. Shen, Z. Ju, X. Tan, E. Liu, Y. Liu, D. Yang, leying zhang, K. Song, L. He, X. Li, sheng zhao, T. Qin, and J. Bian, “PromptTTS 2: Describing and generating voices with text prompt,” in *The 12th International Conference on Learning Representations*, 2024.
- [21] R. Shimizu, R. Yamamoto, M. Kawamura, Y. Shirahata, H. Doi, T. Komatsu, and K. Tachibana, “Prompttts+: Controlling speaker identity in prompt-based text-to-speech using natural language descriptions,” in *Proc. IEEE Int. Conf. Acoust., Speech Signal Process.*, 2024, pp. 12672–12676.
- [22] Z. Chen, X. Liu, E. Cooper, J. Yamagishi, and Y. Qian, “Generating speakers by prompting listener impressions for pre-trained multi-speaker text-to-speech systems,” *CoRR*, vol. abs/2406.08812, 2024.
- [23] Y. Zhang, G. Liu, Y. Lei, Y. Chen, H. Yin, L. Xie, and Z. Li, “Promptspeaker: Speaker generation based on text descriptions,” in *Proc. IEEE Autom. Speech Recognit. Understanding Workshop*, 2023, pp. 1–7.
- [24] J. Hai, K. Thakkar, H. Wang, Z. Qin, and M. Elhilali, “Dreamvoice: Text-guided voice conversion,” *arXiv e-prints*, pp. arXiv–2406, 2024.
- [25] Z. Sheng, Y. Ai, L. Liu, J. Pan, and Z. Ling, “Voice attribute editing with text prompt,” *CoRR*, vol. abs/2404.08857, 2024.
- [26] E. Brochu, N. de Freitas, and A. Ghosh, “Active preference learning with discrete choice data,” in *Annu. Conf. Neural Inf. Process. Syst.*, 2007, pp. 409–416.
- [27] D. C. Kingsley and T. C. Brown, “Preference uncertainty, preference learning, and paired comparison experiments,” *Land Economics*, vol. 86, no. 3, pp. 530–544, 2010.
- [28] Y. Shen, C. Yang, X. Tang, and B. Zhou, “Interfacegan: Interpreting the disentangled face representation learned by gans,” *IEEE Trans. Pattern Anal. Mach. Intell.*, vol. 44, no. 4, pp. 2004–2018, 2022.
- [29] A. Jahanian, L. Chai, and P. Isola, “On the ”steerability” of generative adversarial networks,” in *Proc. Int. Conf. Learn. Represent.*, 2020.
- [30] R. Abdal, P. Zhu, J. Femiani, N. J. Mitra, and P. Wonka, “Clip2stylegan: Unsupervised extraction of stylegan edit directions,” in *Proc. SIG-GRAPH Conf. Comput. Graph. Interactive Tech.*, 2022, pp. 48:1–48:9.
- [31] Z. Wu, D. Lischinski, and E. Shechtman, “Stylegan analysis: Disentangled controls for stylegan image generation,” in *Proc. IEEE Conf. Comput. Vis. Pattern Recognit.*, 2021, pp. 12863–12872.
- [32] Y. Shen, J. Gu, X. Tang, and B. Zhou, “Interpreting the latent space of gans for semantic face editing,” in *Proc. IEEE/CVF Conf. Comput. Vis. Pattern Recognit.*, 2020, pp. 9240–9249.
- [33] E. Härkönen, A. Hertzmann, J. Lehtinen, and S. Paris, “Ganspace: Discovering interpretable GAN controls,” in *Annu. Conf. Neural Inf. Process. Syst.*, 2020.
- [34] N. Spingarn, R. Banner, and T. Michaeli, “GAN ”steerability” without optimization,” in *Proc. Int. Conf. Learn. Represent.*, 2021.
- [35] A. Voynov and A. Babenko, “Unsupervised discovery of interpretable directions in the GAN latent space,” in *Proc. Int. Conf. Mach. Learn.*, vol. 119, 2020, pp. 9786–9796.
- [36] Y. Shen and B. Zhou, “Closed-form factorization of latent semantics in gans,” in *Proc. IEEE Conf. Comput. Vis. Pattern Recognit.*, 2021, pp. 1532–1540.
- [37] W. S. Peebles, J. Peebles, J. Zhu, A. A. Efros, and A. Torralba, “The hessian penalty: A weak prior for unsupervised disentanglement,” in *Proc. Eur. Conf. Comput. Vis.*, ser. Lecture Notes in Computer Science, vol. 12351, 2020, pp. 581–597.
- [38] A. Ramesh, Y. Choi, and Y. LeCun, “A spectral regularizer for unsupervised disentanglement,” *CoRR*, vol. abs/1812.01161, 2018.
- [39] J. Zhu, R. Feng, Y. Shen, D. Zhao, Z. Zha, J. Zhou, and Q. Chen, “Low-rank subspaces in gans,” in *Annu. Conf. Neural Inf. Process. Syst.*, 2021, pp. 16648–16658.
- [40] Y. Wei, Y. Shi, X. Liu, Z. Ji, Y. Gao, Z. Wu, and W. Zuo, “Orthogonal jacobian regularization for unsupervised disentanglement in image generation,” in *Proc. IEEE/CVF Int. Conf. Comput. Vis.*, 2021, pp. 6701–6710.
- [41] J. Kong, J. Kim, and J. Bae, “Hifi-gan: Generative adversarial networks for efficient and high fidelity speech synthesis,” in *Annu. Conf. Neural Inf. Process. Syst.*, 2020.
- [42] K. Qian, Y. Zhang, H. Gao, J. Ni, C. Lai, D. D. Cox, M. Hasegawa-Johnson, and S. Chang, “Contentvec: An improved self-supervised speech representation by disentangling speakers,” in *Proc. Int. Conf. Mach. Learn.*, vol. 162, 2022, pp. 18003–18017.
- [43] A. Baevski, Y. Zhou, A. Mohamed, and M. Auli, “wav2vec 2.0: A framework for self-supervised learning of speech representations,” in *Annu. Conf. Neural Inf. Process. Syst.*, 2020.
- [44] M. Morise, F. Yokomori, and K. Ozawa, “WORLD: A vocoder-based high-quality speech synthesis system for real-time applications,” *IEICE Trans. Inf. Syst.*, vol. 99-D, no. 7, pp. 1877–1884, 2016.
- [45] B. Desplanques, J. Thienpondt, and K. Demuyck, “ECAPA-TDNN: emphasized channel attention, propagation and aggregation in TDNN based speaker verification,” in *Proc. Interspeech*, 2020, pp. 3830–3834.
- [46] Y. Koizumi, H. Zen, S. Karita, Y. Ding, K. Yatabe, N. Morioka, M. Bacchiani, Y. Zhang, W. Han, and A. Bapna, “Libritts-r: A restored multi-speaker text-to-speech corpus,” in *Proc. Interspeech*, 2023, pp. 5496–5500.
- [47] H. Zen, V. Dang, R. Clark, Y. Zhang, R. J. Weiss, Y. Jia, Z. Chen, and Y. Wu, “Libritts: A corpus derived from librispeech for text-to-speech,” in *Proc. Interspeech*, 2019, pp. 1526–1530.
- [48] J. Kim, J. Kong, and J. Son, “Conditional variational autoencoder with adversarial learning for end-to-end text-to-speech,” in *Proc. Int. Conf. Mach. Learn.*, vol. 139, 2021, pp. 5530–5540.
- [49] S. J. Wright, “Coordinate descent algorithms,” *Math. Program.*, vol. 151, no. 1, pp. 3–34, 2015.
- [50] J. Yamagishi, C. Veaux, S. King, and S. Renals, “Speech synthesis technologies for individuals with vocal disabilities: Voice banking and reconstruction,” *Acoust. Sci. Technol.*, vol. 33, no. 1, pp. 1–5, 2012.
- [51] R. A. Horn and C. R. Johnson, *Matrix Analysis*, 2nd ed. Cambridge: New York: Cambridge University Press, 2013.
- [52] M. Ester, H. Kriegel, J. Sander, and X. Xu, “A density-based algorithm for discovering clusters in large spatial databases with noise,” in *Proc. Int. Conf. Knowl. Discovery Data Mining*, 1996, pp. 226–231.